CHALMERS
UNIVERSITY OF TECHNOLOGY

Adaptive inverse analysis (AIA) applied and verified on various fiber reinforced concrete composites

Materials and Structures (2018)51:60
https://doi.org/10.1617/s11527-018-1177-0

ORIGINAL ARTICLE

Adaptive inverse analysis (AIA) applied and verified on various fiber reinforced concrete composites

Michael S. Jepsen · Lars Damkilde · Ingemar Lövgren · Carlos Berrocal

Received: 16 July 2017 / Accepted: 19 March 2018

Abstract During the past decades several inverse approaches have been developed to identify the stress-crack opening ($\sigma - w$) by means of indirect test methods, such as the notched three point bending-, wedge splitting-, and round panel testing. The aim is to establish reliable constitutive models for the tensile behavior of fiber reinforced concrete materials, suitable for structural design. Within this context, the adaptive inverse analysis (AIA) was recently developed to facilitate a fully general and automatized inverse analysis scheme, which is applicable in conjunction with analytical or finite element simulation of the experimental response. This paper presents a new formulation of the adaptive refinement criterion of the AIA method. The paper demonstrates that the refinement criterion of the nonlinear least square curve fitting process, is significantly improved by coupling the model error to the crack mouth opening and the crack opening displacement relationship ($w_{\mathrm{cmod}} - w_{\mathrm{cod}}$). This enables an adaptive refinement of the $\sigma - w$ model in the line segment with maximum model error, which entails significant improvement of the numerical efficiency of the AIA method without any loss of robustness. The improved method is applied on various fiber reinforced concrete composites and the results are benchmarked with the inverse analysis method suggested by the Japanese Concrete Institute (Method of test for fracture energy of concrete by use of notched beam, Japanese Concrete Institute Standard, Tokyo, 2003) and recently adopted in ISO 19044 (Test methods for fibre-reinforced cementitious composites—load-displacement curve using notched specimen, 2015). The benchmarking demonstrates that the AIA method, in contradiction to the JCI/ISO method, facilitates direct determination of the tensile strength and operational multi-linear $\sigma - w$ models.

Keywords Fiber reinforced concrete · Adaptive inverse analysis · Post cracking behavior · Multi-linear cohesive models · Least square curve fitting

1 Introduction

Since the pioneering work of Hillerborg et al. [1], who suggested that the crack propagation in cementitious materials is governed by the stress versus crack opening relationship, several research campaigns have been dedicated to reveal the post cracking behavior of plain or fiber reinforced concretes. The fictitious crack model as formulated by Hillerborg et al., is governed

M. S. Jepsen (✉) · L. Damkilde
Department of Civil Engineering, Aalborg University, Niels Bohrs Vej 8, 6700 Esbjerg, Denmark
e-mail: msj@civil.aau.dk

I. Lövgren · C. Berrocal
Department of Civil and Environmental Engineering, Chalmers, Sven Hultins Gata 8, Göteborg, Sweden
e-mail: cosil@chalmer.se

Published online: 24 April 2018

by the direct tensile strength, Youngs modulus and the cohesive model, which relates the fictitious crack opening to the crack stresses ($\sigma - w$) transferred between the crack faces. The governing parameters can explicitly be determined by direct tensile testing, see e.g. Petersson [2] and RILEM TC 162-TDF [3], who emphasize that this test method ideally provides the tensile constitutive model, but the demand for controlled and stable crack growth is difficult to achieve in practice. Consequently much effort has been directed toward establishing indirect test methods, which are kept sufficiently simple to be performed in any laboratory.

For plain concrete, the measure of the fracture energy is of key importance, while the actual shape of the $\sigma - w$ curve is of significance for the design of fiber reinforced concrete members. Thus several test methods have been developed for fracture mechanical testing of concretes. Basically, any test specimen can fulfill this purpose, as long as the boundary conditions are clearly defined and it secures a stable propagation of a mode I crack. Test specimens, such as the notched three point bending test (3PBT), the wedge splitting test (WST) and recently the round panel test (RPT), among others, have been used as indirect test methods for plain as well as fiber reinforced concretes. Each method has advantages and drawbacks, see e.g. Østergaard et al. [4], and no actual consensus exists for the indirect test methods. However, the trend is that the notched 3PBT is the preferred indirect test method and has been standardized in e.g. JCI [5] and ISO [6] codes and AFGC recommendation [7].

The inverse determination of the tensile constitutive relationship relies generally on the fitting of a response from the corresponding mechanical model to the measured response. The parameters which constitute the $\sigma - w$ need to be known a priori in this process, because they are employed as governing fitting variables. The fitting process is performed by adjusting the $\sigma - w$ model until a minimum discrepancy between model and measurement is obtained, hence the resulting $\sigma - w$ model expresses an average model for the given data range. This curve fitting approach was originally suggested by Roelfstra and Wittmann [9], who used finite element simulation of the notched 3PBT, where the fracture parameters of the bi-linear $\sigma - w$ model were applied as governing fitting variables. The method has later been used in combination with analytical formulations for crack propagation in concrete beams. The analytical models are desirable, because they reduce the computation time considerably, compared to the finite element solution, cf. Slowik et al. [10]. The analytical approach has been the basis of the work in Sousa and Gettu [11], Østergaard et al. [12], Stephen et al. [13] and Reddy et al. [14].

In the design of fiber reinforced concrete structures, the shape of the $\sigma - w$ model is of key importance to analyse the force-displacement, moment-curvature, or moment—crack opening response in service conditions. Thus high accuracy of the cohesive model is needed, and consequently the assumption of a simple bi-linear $\sigma - w$ model is not sufficient to capture the structural response accurately. This is especially the case in the crack opening range of [0;0.5 mm], which is the crack width opening limit in the serviceability limit state. Generally, the formulation of the analytical approaches makes it difficult to use a multi-linear formulation of the tensile constitutive model, as shown in Skocek et al. [15]. Kitsutaka [16, 17], suggested a method where the shape of the constitutive model is not to be defined a priori. The idea is to fit the simulated response to the measured response point by point, using a multi-linear formulation of the cohesive model, as sketched in Fig. 1a. Kitsutaka [16] originally formulated the stepwise method for the notched 3PBT experiment and the corresponding response model was formulated as a finite element problem. The stepwise procedure has later been adopted in the inverse analysis of RPT and 3PBT in conjunction with an analytical formulation of the response models, see e.g. Nour et al. [18] and Montaignac et al. [19]. The drawbacks of the method is the fact that the material properties are assumed homogeneous along the crack path. Accordingly, the method may not be used for determining the direct tensile strength as pointed out in Löfgren et al. [20]. The method is, due to the incremental determination of the $\sigma - w$ model, very sensitive to the mechanical behavior at crack initiation, where a bundle of fibers in the first layer of cracked concrete can cause an overestimation of the tensile strength and influence the initial slope of the cohesive model.

In the light of these issues, the AIA method was developed by Jepsen et al. [8]. The method is based on least square curve fitting and facilitates multi-linear $\sigma - w$ models, which are obtained without a priori knowledge of the final $\sigma - w$ model. Accordingly, the

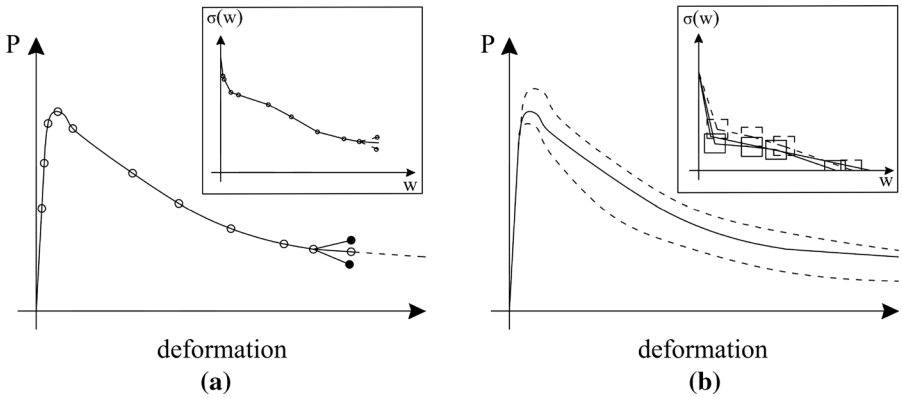

Fig. 1 **a** Stepwise method [5] and **b** AIA method [8]

issues related to local material in-homogeneity do not affect the cohesive model in average, because the fitting procedure treats the global deflection response. The multi-linear cohesive model is achieved by means of the adaptive formulation of the fitting scheme, which prevents local minimum problems in the curve fitting process. The local minimum problem is avoided by constraining the search for optimum of each fitting variable, as illustrated in Fig. 1b. Between every iteration the feasible search region for each variable is updated. If a minimum (tol $< 1\%$) of change in the entire set of variables is reached, a new point on the cohesive model is created on the line segment with maximum length. Thus the next curve fitting iteration contains an extra set of variables and before proceeding the curve fitting process, the feasible search regions are recomputed for all variables. This successive addition of variables is the basis for the AIA method and this provide a robust curve fitting method that avoids local minimum problems.

This paper will in continuation to the AIA method presented in Jepsen et al. [8] provide a new formulation of the refinement method used in the adaptive curve fitting process. The previously suggested refinement method facilitates high robustness, but lacks computational efficiency. The paper therefore presents a new refinement method, which facilitates a significantly improved convergence rate of the AIA method, without changing the high numerical robustness. Subsequently the efficiency and robustness are evaluated for various types of fiber reinforced concretes compositions. The results are benchmarked to the stepwise method as developed by Kitsutaka [16] and Ucida et al. [21] later proposed as the standard inverse analysis procedure in the Japanish code [5] and most recently in the ISO standard [6].

2 The adaptive inverse analysis method

This section first provides a brief introduction to the general principles of the AIA method and subsequently presents the reformulation of the refinement criterion used in the adaptive curve fitting process. The AIA method is based on non-linear least-square curve fitting techniques and in general facilitates a fully automated inverse analysis approach, which provide very accurate and non-biased multi-linear cohesive models, Jepsen et al. [8].

2.1 Numerical procedure

The adaptive inverse analysis is initiated by fitting the simulated response by means of a simple linear cohesive model containing 3 line segments. Each set of fitting variables is constrained by a feasible search region. The interpretation of the fitting variables and their feasible search regions is illustrated in Fig. 2. It is seen that the governing fitting variables are $\{\sigma_i, w_i f_t\}$ and their feasible search region is computed by Eq. 1.

$$\begin{aligned} f_{t,\mathrm{lim}} &= f_t \pm \delta_{f_t} \\ w_{i,\mathrm{lim}} &= w_i \pm \eta\delta_{w,i} \\ \sigma_{i,\mathrm{lim}} &= \sigma_i \pm \eta\delta_{\sigma,i} \end{aligned} \tag{1}$$

where the δ parameter designates the distance to the nearest boundary condition, which identify the feasible search region for the given parameter, see Fig. 2 and for computational details see Jepsen et al. [8]. The

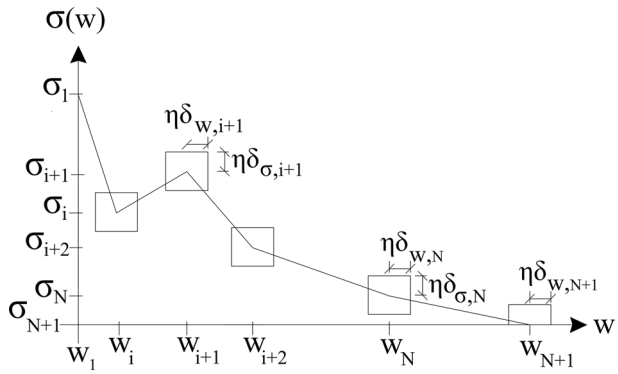

Fig. 2 Basic parameters of the multi-linear $\sigma - w$ relationship

fitting variables are constrained by these search regions during the entire curve fitting process, which secures a robust search for optimal fit. The size of the search region, cf. Fig. 2, is efficiently controlled by the δ and η parameters, where η controls the final size of the search region. In the current work, η has been set to 1/3, which secures a sufficient reduction of the search region, as suggested in Jepsen et al. [8]. The process is continued until the best fit has been identified for the given model and the active search region. If none of the variables have changed more than 1 % since the previous search region adjustment, a new line segment is introduced to the $\sigma - w$ model. This is the adaptive part of the inverse analysis, and the optimization process is continued with a model containing an extra set of variables, σ_i, w_i. In the AIA method developed in Jepsen et al. [8] the new point is added on the line segment with maximum distance between the two points constituting the line segment. The original formulation of the refinement method is very robust, but has insufficient computational efficiency. It is therefore suggested to utilize that the formulation of the mechanical problem makes it possible to improve the formulation of the refinement criterion.

2.2 New refinement method

The general idea is to compute an error function, which is a measure of the error between the measured and the simulated response, as function of the crack mouth opening displacement w_{cmod}, cf. Fig. 3. The model error is determined as the absolute relative deviation between the measured and the fitted response curve. It is suggested to divide the model error into two zones, representing the elastic zone (zone I) and the crack propagation zone (zone II). Only the model error in zone II will be treated in this paper.

Both finite element and analytical simulation of the mechanical problem facilitate computation of the crack mouth opening response, w_{cmod}, of the notch and the crack opening response at the tip of the notch, w_{cod}. This enables a direct coupling between the computed model error and the crack opening displacement, w_{cod}, as sketched in Fig. 3. The w_{cod} with maximum error between measured and simulated data is in this way determined. The w_{cod} can be related directly to the $\sigma - w$ and it is thus possible to determine the line segment in the $\sigma - w$ model that contains the maximum model error and directly refine the $\sigma - w$ model in the region with greatest influence on the model error reduction.

3 Basis for the performance evaluation

The following section outlines the method chosen for evaluating the performance of the AIA method, as defined in the previous section. The purpose is to evaluate the performance by means of several application examples, where the robustness and computational efficiency are monitored. Thus the following section describes the configuration of the inverse analysis.

3.1 Experimental setup

In this paper the notched beam subjected to three point bending is used, because it is well developed in codes and recommendations, ASTM [22], JCI [5], ISO [6], AFGC [7], RILEM [23]. In this paper the specimen suggested by RILEM [23] is used for testing. To

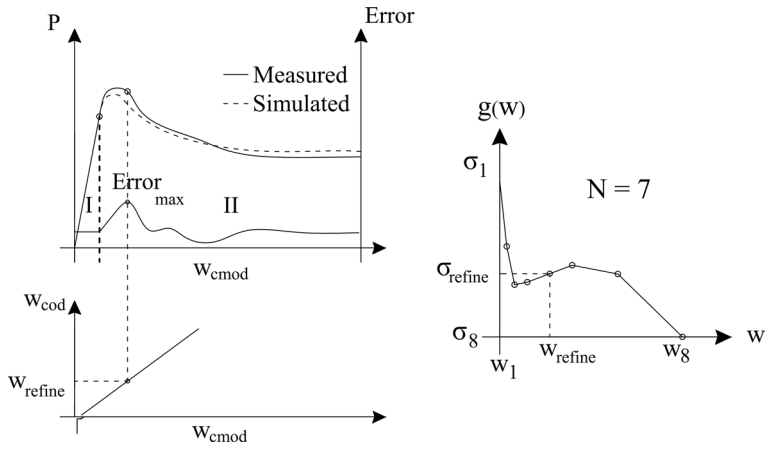

Fig. 3 Error as function of deformation

secure stable crack growth, the tests are carried out by closed loop control of w_{cmod}, which are measured by a clip gauge mounted 8 mm from the bottom surface of the beam.

3.2 Experimental program

Four different concrete compositions is used for the performance testing of the AIA method, cf. Table 1. The experiments have previously been presented in Berrocal et al. [24] (Mix 1–2) and Löfgren et al. [20] (Mix 3–4). 5 Notched beam specimens with an approximately compressive strength of 60 MPa has been prepared for each concrete mixture. It is chosen to use the mean response curve for each mixture, such that the influence from non-homogeneous distribution of the fibers is minimized in the response used for the inverse analysis. Different types of fiber materials, such as PVA and steel fibers have been used. Furthermore, the length of the fibers has been varied. The concretes were designed to be self compacting—providing good workability despite of the fiber addition.

Table 1 Composition * after Berrocal et al. [24], composition ** after Löfgren et al. [20]

Constituents	Mix 1*(kg/m^3)	Mix 2* (kg/m^3)	Mix 3** (kg/m^3)	Mix 4** (kg/m^3)
Cement (CEM I 42.5N SR3 MH/LA)	360	360	–	–
Cement (CEM II/A-LL 52.5R)	–	–	360	360
Limestone filler (Limus 40)	165	165	–	–
Fly ash	–	–	100	100
Effective water	169	169	172	172
Aggregate 0–4 mm	770	770	745	745
Aggregate 4–8 mm	–	–	312	312
Aggregate 4–16 mm	833	833	634	634
Superplasticizer—Glenium 51/18	5.76	5.76	–	–
Superplasticizer—Siksa ViscoCrete 34	–	–	0.4	0.4
Air entrainer–MicroAir 105	0.72	0.72	–	–
Air content			1.5	1.5
Fiber properties Vol%				
Steel—Dramix© (65/35)	0.5	–	–	1.0
Steel—Dramix© (65/60)	–	–	1.0	–
PVA—KuralonTM *RF*4000 (18/90)	–	0.75	–	–

3.3 Experimental results

The average response curves of the notched three point beam testing is seen in Fig. 4. The tests shows that the coefficient of variation is approximately 15% for test series 1–3, while test series 4 have a coefficient of variation of 8%. In mixture 1 and 2 the same concrete composition is used, while the fiber material and aspect ratio are varied. Comparing the experimental results of these two mixtures, it is clearly seen that the steel fiber reinforcement used in mixture 1 enhances the post-cracking response significantly, compared to results obtained by mixture 2, which was reinforced by PVA fibers. This indicates that a significantly higher volume of synthetic fibers is needed to achieve the same post-cracking properties. Mixture 3 and 4 consist of the same concrete composition and reinforced with the same steel fiber volume. Here the length of the fibers is varied, and similar peak-force and post-cracking behavior are seen, cf. Fig. 4.

3.4 Mechanical model and simulation method

The simulation method chosen in this paper was previously developed in Jepsen et al. [8], and is based on the nonlinear cracked hinge model, developed in Ulfkjær et al. [25], Pedersen [26] and Olesen [27]. The analytical model has been benchmarked to e.g. numerical simulation in DIANA, see e.g. Löfgren [28] and Østergaard [12], RILEM [29], which shows good performance of the model. For further details about the simulation method, the reader is recommended to consult the work in Jepsen et al. [8].

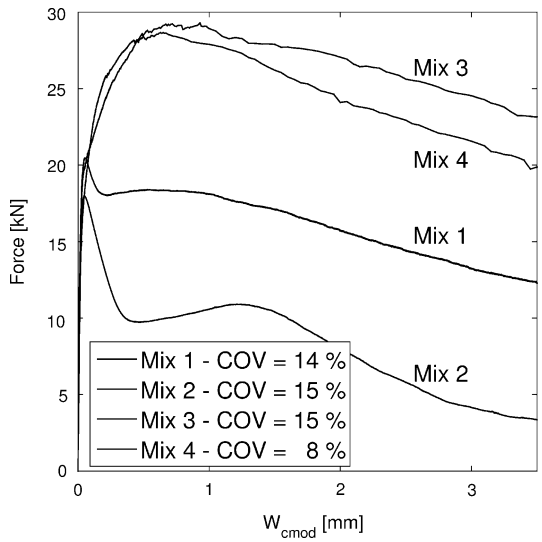

Fig. 4 Average response curve of test series 1–4

4 Performance: new refinement method

To evaluate the performance of the new refinement method, a comparison of the convergence rate of the original and the new AIA method will be presented. Typically, it is sufficient to use the least square residuals as measure of the convergence rate during the curve-fitting process. However, it is suggested to employ a more objective approach, in terms of the Coefficient of Variation (CoV) and Bias of the ratios between the measured and simulated response. In the following are the CoV and Bias only computed for the data range after crack initiation (Zone II). The target for the optimal inverse result is thus a CoV approaching 0 and a Bias approaching 1. This method provide direct information about the system error, in terms of Bias. Thus the final curve fit must satisfy Bias ≈ 1.

Adopting the CoV and Bias measure in the AIA algorithm entail that these parameters are evaluated at each search region re-computation, hence when the curve fit reaches optimal fit within the respective search region is the CoV and Bias computed by Eq. 2.

$$\begin{aligned} r_i &= \frac{P_{\mathrm{sim},i}}{P_{\mathrm{meas},i}} \\ \mu &= \frac{\sum_{i=1}^{N} r_i}{N} \\ s &= \sqrt{\frac{1}{N}\sum_{i=1}^{N}(r_i-\mu)^2} \\ \mathrm{CoV} &= \frac{s}{\mu} \end{aligned} \tag{2}$$

where r_i, is the ratio between the simulated force P_{sim} and the measured force P_{meas}, μ is the mean value of the ratios (Bias), s is the standard deviation of the ratios, and finally the CoV is the Coefficient of Variation between the simulated and measured $P - w_{\mathrm{cmod}}$.

To examine the performance of the new refinement method, the result from the inverse analysis of Mix 4 is used. The comparison is conducted on data in the range of $w_{\mathrm{cmod}} = [0;1\ \mathrm{mm}]$. The only difference between the compared methods are thus related to the refinement criterion in use. The results of this

comparison are seen in Fig. 5a and illustrates the convergence rate during the curve fitting process, where each iteration represents a curve fit process where the fitting variables are constrained by a given search region. The curve fitting process within this feasible search region is continued until either the optimality criterion for each variable, (tol = 1e−6) or the maximum number of sub-iterations is reached (it = 25).

Figure 5a shows the convergence rate of the new and previous refinement criterion. It is observed that the convergence rate is significantly increased by the new refinement method, which is furthermore substantiated by comparing the number of model evaluations used in the curve fitting process. According to Fig. 5b is the number of model evaluations approximately the same for each iteration, hence the new refinement method provide improved convergence for the same number of model evaluations.

5 Benchmarking between the AIA and JCI method

The resulting curve fit of the inverse analysis is seen in Fig. 6, where both the result from the AIA method and JCI method are presented. To conduct a detailed benchmarking between the AIA and JCI/ISO inverse methods, the results of Mix 2 and 4 are chosen for exemplification. In Figs. 7 and 8 are the resulting curve fit and the corresponding inversely determined $\sigma - w$ models illustrated. In the JCI/ISO method, the model error tolerance is recommended as 5% to secure a stable solution. By comparing the two inverse

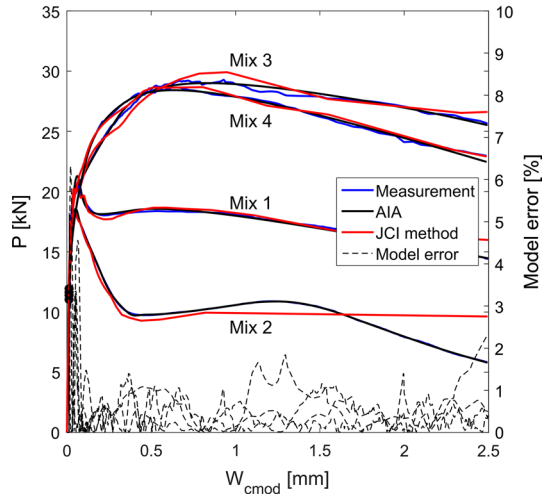

Fig. 6 $P - w_{\text{cmod}}$ estimated by AIA and JCI method for all mixtures

methods, it is observed that the JCI method is very sensitive to local effects and does not estimate the direct tensile strength accurately. The two methods are converging at crack openings above 0.2–0.25 mm, where the initial effects of crack initiation are decreasing. It is noticed that the AIA method provides significantly more operational $\sigma - w$ models ready for structural design analysis, whereas the $\sigma - w$ models determined by the JCI method have to be filtered. Figure 9 presents a zoom plot and it shows the behavior of the two models at crack openings below 0.5 mm. This branch is critical for service limit state calculations and thus operational $\sigma - w$ models are needed, which the AIA method provides directly.

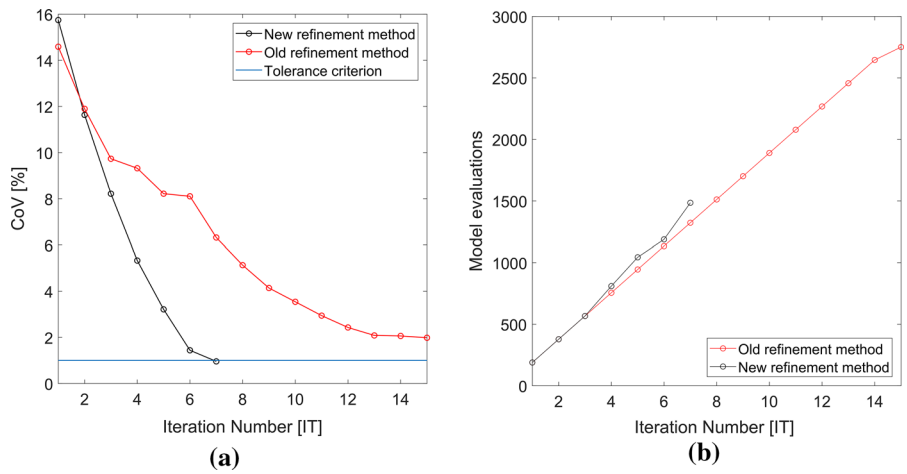

Fig. 5 Comparison between the old and the new refinement method, **a** convergence rate, **b** model evaluations

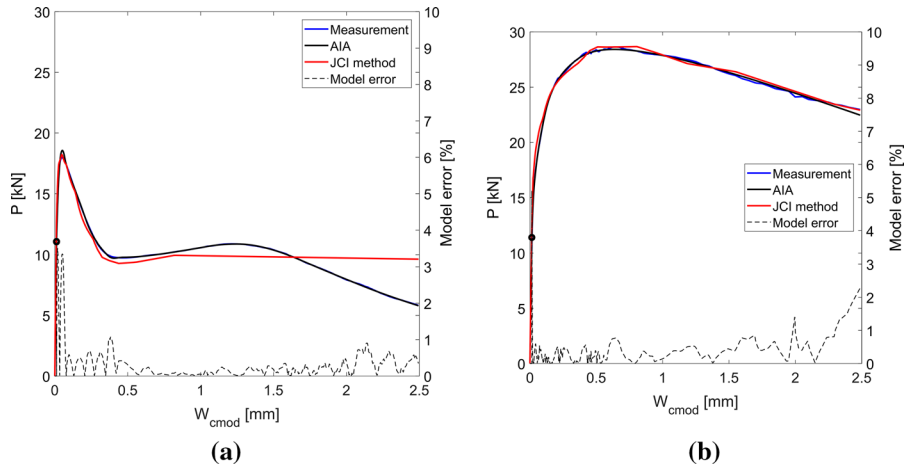

Fig. 7 $P - w_{\mathrm{cmod}}$ from AIA and JCI method for mixture 2 and 4

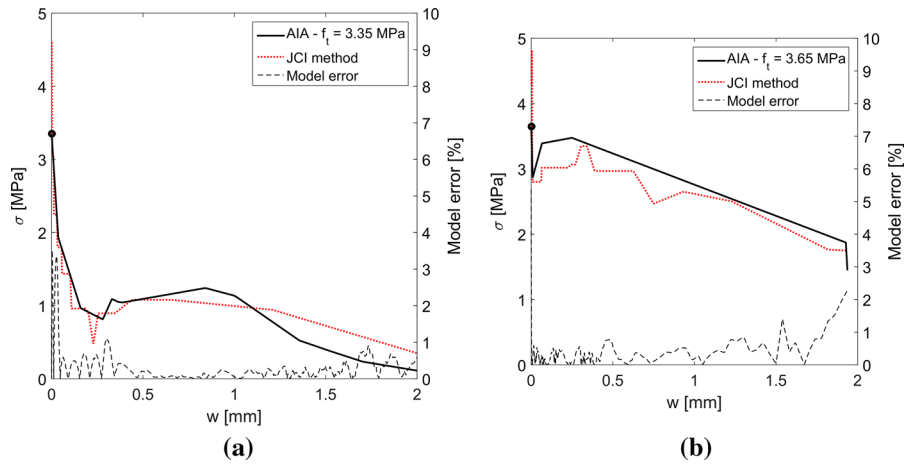

Fig. 8 $\sigma - w$ from AIA and JCI method for mixture 2 and 4

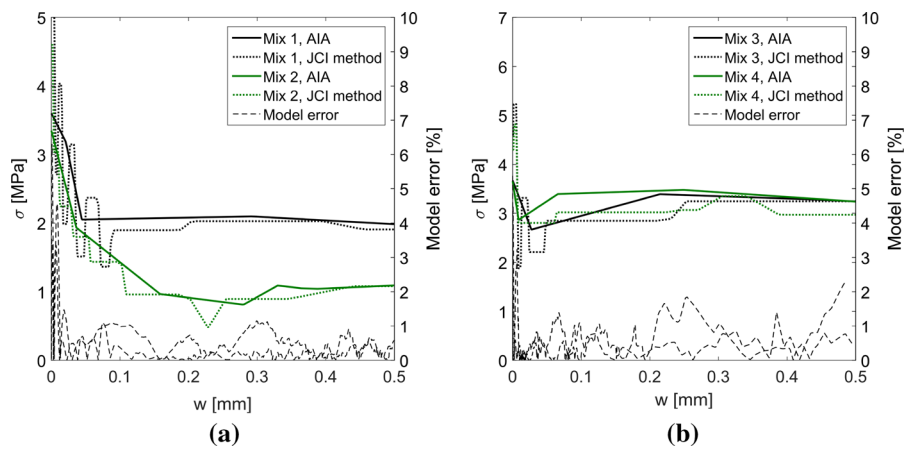

Fig. 9 Zoom of the resulting cohesive models in the range [0:0.5 mm]

The model error function for the final fit from the AIA method is illustrated in Fig. 6. It is noticed that the model error is relatively high in the branch between the elastic zone (zone I) and crack initiation (zone II). Due to the coupling between w_{cmod} and w_{cod} in the analytical model, it is possible to identify the

model error in the $\sigma - w$ model as well, cf. Figs. 7 and 8. Here it is seen that the maximum model error is observed within 0.1 mm of the crack opening displacement.

5.1 Result evaluation: AIA method

The convergence rate is evaluated for all the test series in Fig. 10a and it is seen that the AIA method converges at approximately 10 iterations (feasible search region re-computations). In addition to this observation, it is of great interest to study the model order (N) required to obtain a certain curve fit. Such study provide information of the complexity of the $\sigma - w$ model needed to describe the postcracking behavior of a given material. The evaluation of the model order is exemplified by the inverse analysis of Mix 2 and 4, cf. Fig. 10b. It is shown that the $\sigma - w$ model converges at an order of approximately $N = 6$. The high order model is primary caused by the initial part of the $\sigma - w$ curve, in the range from crack initiation to $w = 0.3$ mm. This observation is interesting, because simple bi-linear $\sigma - w$ models are often seen as sufficient to estimate the crack opening in the service limit state, where the crack width does not exceed 0.3 mm. Figure 9 shows that high order models ($N > 2$) is essential for predicting the initial stage of crack propagation, where the crack opening behaviour is governed by activation of the fiber bridging effect.

Table 2 presents the evaluation of the final $\sigma - w$ models obtained by the AIA method. The evaluation is mainly performed on the data from Zone II (Post-cracking range), because the Young's modulus is a fixed parameter during the curve fitting process. Table 2 shows that the final models are non-biased and furthermore characterized by very low CoV ≈ 1. Although the linear elastic zone is not part of the curve-fitting process, it is possible to compute the maximum deviation (Model error) between the simulated and measured curve in the entire data range (Zone I + II), as illustrated in Fig. 6. The maximum model error for all $\sigma - w$ models is limited to a narrow region, immediately after crack initiation and is in the range of 4–7%.

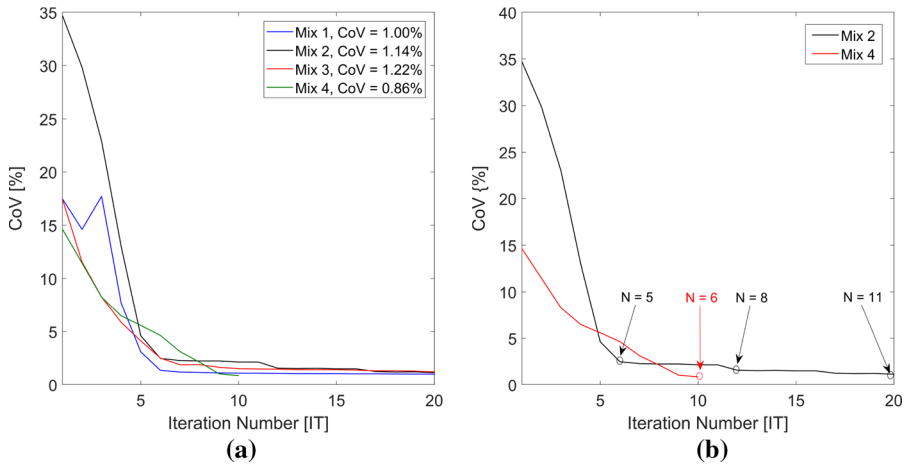

Fig. 10 **a** Convergence rate for all mixtures, **b** convergence rate and model order for mixture 2 and 4

Table 2 Model error, CoV and Bias of the final $\sigma - w$ models obtained by the AIA method

Concrete type	Max. model error (%)	Bias (ratio)	CoV (%)	N_{stop} (Order)
Mixture 1	6.3	1.00	1.00	11
Mixture 2	7.1	1.00	1.09	11
Mixture 3	4.5	1.00	1.21	12
Mixture 4	6.6	1.00	0.86	5

6 Conclusion

The paper presents a new refinement criterion for the Adaptive Inverse Analysis (AIA) method, which aims at improving the computational efficiency of the curve fitting process. The computational efficiency is compared to the original refinement method and it is demonstrated how the new refinement criterion improves the convergence rate of the curve fitting problem significantly. The new AIA method is furthermore benchmarked to the step-wise inverse method suggested by JCI [5] and ISO [6]. The performance of both methods is tested and compared for various types of fiber reinforced concretes. The benchmarking demonstrate that the AIA method provides very operational $\sigma - w$ curves for practical design in the service limit state, compared to the JCI method. Tests shows that it is possible to obtain $\sigma - w$ models with a bias of 1.00 and CoV in the range 1–2% for models of order $N = 6$. It is concluded that the new refinement method improves the computational efficiency without any loss of numerical robustness of the AIA method. In addition to this, it is concluded that the adaptive inverse analysis method provides accurate curve fits and non-biased multi-linear $\sigma - w$ models, which are directly operational in structural design analysis of fiber reinforced concrete structures.

Compliance with ethical standards

Conflict of interest The authors declare that they have no conflict of interest.

References

1. Hillerborg A, Moder M, Petersson PE (1976) Analysis of crack formation and crack growth in concrete by means of fracture mechanics and finite element. Cem Concr Res 6:773–782
2. Petersson PE (1981) Crack growth and development of fracture zone in plain concrete and similar materials. Ph.D. Dissertation, Report TVBM-1006, Division of Building Materials, Lund Institute of Technology
3. RILEM-TC-162-TDF (2001) Uni-axial tension test for steel fibre reinforced concrete. Mater Struct 34:3–6
4. Østergaard L, Olesen JF (2004) Comparative study of fracture mechanical test methods for concrete. Fract Mech Concr Struct 11:455–462 (**Victor Li (ed). IA-FraMCoS, USA**)
5. JCI-S-001-2003 (2003) Method of test for fracture energy of concrete by use of notched beam. Japanese Concrete Institute Standard, Tokyo
6. ISO 19044:2016 (2016) Test methods for fibre-reinforced cementitious composites – Load-displacement curve using notched specimen, ISO/TC 71/SC 6 Non-traditional reinforcing materials for concrete structures
7. AFGC Recommendation (2013) Ultra high performance fibre-reinforced concretes. Association Francaise de Génie Civil
8. Jepsen MS, Damkilde L, Lövgren I (2016) A fully general and adaptive inverse analysis method for cementitious materials. Mater Struct RILEM (**online published**)
9. Roelfstra PE, Wittmann FH (1986) Numerical method to link strain softening with failure of concrete. In: Fracture toughness and fracture energy of concrete. Development in Civil Engineering, vol 18. Elsevier, pp 163–175
10. Slowik V, Villmann B, Bretschneider N, Villmann T (2005) Computational aspects of inverse analysis for determining softening curves of concrete. Comput Methods Appl Mech Eng 195:7223–7236
11. Sousa JLA, Gettu R (2006) Determining the tensile stress-crack opening curve of concrete by inverse analysis. J Eng Mech 132:141–148
12. Østergaard L (2003) Early-age fracture mechanics and cracking of concrete—experiments and modelling. Ph.D. Dissertation, Department of Civil Engineering, Technical University of Denmark
13. Stephen JS, Gettu R, Raphael R (2016) Effect of loading rate on the fracture behavior of fibre reinforced concrete. In: Saouma V, Bolander J, Landis E (eds) 9th international conference on fracture mechanics of concrete and concrete structures, Proceedings FraMCoS-9. https://doi.org/10.21012/FC9.071
14. Reddy KC, Subramaniam KVL (2016) Analysis for multi-linear stress-crack opening cohesive relationship: application to macro-synthetic fiber reinforced concrete. Eng Fract Mech 169:128–145. https://doi.org/10.1016/j.engfracmech.2016.11.015
15. Skocek J, Stang H (2008) Inverse Analysis of the Wedge-splitting test. Engineering Fracture Mechanics 75:3173–3188
16. Kitsutaka Y (1995) Fracture parameters for concrete based on poly-linear approximation analysis of tension softening diagram. In: Wittmann FH (ed) Fracture mechanics of concrete structures, Proceedings FRAMCOS-2
17. Kitsutaka Y (1997) Fracture parameters by polylinear tension-softening analysis. J Eng Mech 123:444–50
18. Nour A, Massicotte B, de Montaignac R, Charron J-P (2015) Development of an inverse analysis procedure for the characterisation of softening diagrams for FRC beams and panels. Constr Build Mater 94:35–44
19. de Montaignac R, Massicotte B, Charron J-P, Nour A (2011) Design of SFRC structural elements: post-cracking tensile strength measurements. Mater Struct RILEM 45:609–622
20. Löfgren I, Stang H, Olesen JF (2005) Fracture properties of FRC determined through inverse analysis of wedge splitting and three-point bending tests. J Adv Concr Technol 3:423–434
21. Uchida Y, Kurihara N, Rokugo K, Koyanagi W (1995) Determination of tension softening diagrams of various kinds of concrete by means of numerical analysis. In: Wittmann FH (ed) Fracture mechanics of concrete structures, FRAMCOS-2, pp 17–30

22. ASTM C 1018 (1992) Standard test method for flexural toughness and first crack strength of fiber-reinforced concrete (using beam with Third-point loading). In: ASTM C 1018-92, ASTM annual book of standards, vol 04.02. pp 510–516
23. RILEM-TC-162-TDF (2002) Bending test. Mater Struct 35:579–582
24. Berrocal CG, Löfgren I, Lundgren K, Tang L (2015) Corrosion initiation in cracked fibre reinforced concrete: influence of crack width, fibretype and loading conditions. Corros Sci 98:128–139
25. Ulfkjær JP, Brincker R, Krenk S (1990) Analytical model for moment-rotation curves if concrete beams in bending fracture behavior and design of materials and structures. In: Firrao D (ed) Proceedings of 8th conference on fracture-ECF8, engineering materials advisory services LTD, vol 2. pp 612–617
26. Pedersen C (1996) New production processes, materials and calculation techniques for fiber reinforced concrete pipes. Ph.D. Dissertation. Department of Structural Engineering and Materials, Technical University of Denmark
27. Olesen JF (2001) Fictitious crack propagation in fiber-reinforced concrete beams. J Eng Mech 127:272–280
28. Löfgren I (2005) Fibre-reinforced concrete for industrial construction—a fracture mechanics approach to material testing and structural analysis. Ph.D. Dissertation, Chalmers University of Technology
29. RILEM-TC-162-TDF (2002) Design of fiber reinforced concrete using the $\sigma - w$ method: principles and applications. Mater Struct 35:262–278